ChemComm

COMMUNICATION

View Article Online
View Journal | View Issue

Cite this: *Chem. Commun.*, 2023, 59, 11516

Received 20th July 2023,
Accepted 4th September 2023

DOI: 10.1039/d3cc03487a

rsc.li/chemcomm

Triazine pyridinium derivative supramolecular cascade assembly extended FRET for two-photon NIR targeted cell imaging†

Xuan Zhao, Xiaolu Zhou, Wen-Wen Xing and Yu Liu *

A triazine pyridinium derivative (TAZpy) was encapsulated into the cavity of a cucurbit[7]uril and further assembled with sulfonatocalix[4]-arene, hyaluronic acid and commercial dyes, which not only achieved fluorescence cascade enhancement and an effective FRET process based on macrocyclic confinement, but was also applied in two-photon NIR targeted cell imaging.

The construction of supramolecular cascade assemblies based on macrocycle confined guest chromophores promoting luminescence behaviour has been a research hotspot, which is widely applied in the fields of biological imaging, energy transfer, information anticounterfeiting and luminescent materials.[1] Many research studies have been reported on macrocyclic confinement to modulate photophysical behaviors.[2] In particular, the aggregation-caused quenching guest molecules are tightly encapsulated into the cavity of macrocyclic hosts, such as cyclodextrins, pillararenes, and cucurbiturils, which can alter the packing modes and restrict molecular rotation with an effective improvement in luminescence performance.[3] Moreover, the supramolecular cascade assemble strategy based on macrocyclic confinement has also been rapidly developed to further extend the process of phosphorescence and Förster resonance energy transfer (FRET).[4] For example, George *et al.* reported that a phthalimide phosphor was encapsulated by cucurbit[7]uril (CB[7]) and assembled with negatively charged laponite, which showed room-temperature phosphorescence with high quantum yield in aqueous solution and was used as an efficient light-harvesting energy transfer scaffold for commercial fluorescent dyes.[5] Our group reported configurationally confined supramolecular cascade assemblies based on the tetraphenylethylene pyridinium, CB[8] and sulfobutylether-β-cyclodextrin through electrostatic and host–guest interaction, which could change the topological morphology from nanoparticles to nanosheets and then exhibited strong near-infrared (NIR) fluorescence emission with high energy transfer efficiency of 75% by doping the dye AlPcS4, applicable in the storage of multicolor luminescence information and a variety of logical gate systems.[6] However, the regulation of topological morphology enhanced fluorescence emission through supramolecular cascade assembly based on macrocyclic confinement remains a formidable challenge, especially in two-photon excitation and NIR emission.

Herein, we report a supramolecular cascade assembly achieving NIR fluorescence emission for two-photon targeted cancer cell imaging (Scheme 1). The vinyl pyridinium modified triazine derivative (TAZpy) first formed a 1 : 3 stoichiometric inclusion complex with CB[7] *via* host–guest interaction, and the green fluorescence emission at 510 nm was enhanced in aqueous solution due to the macrocyclic confinement. The amphiphilic sulfonatocalix[4]arene (SC4AD) co-assembled with the TAZpy-CB[7] complex by electrostatic interaction and then formed nanofibers with further increased fluorescence intensity. Furthermore, the SC4AD-TAZpy-CB[7] cascade assembled with targeting agent hyaluronic acid (HA), which not only transformed the topological morphology from nanofibers into nanoparticles but also obtained a relatively strong fluorescence emission at 510 nm. The cascade formed supramolecular nanoparticles HA-SC4AD-TAZpy-CB[7] possessing a tight internal hydrophobic structure were considered an excellent FRET platform. Benefiting from the sufficient overlap between the fluorescence emission region of HA-SC4AD-TAZpy-CB[7] and the absorption band of RhB, the first-step energy transfer process was realized. Then, through doping the secondary Nile blue dye (NiB) into the above systems, the second-step energy transfer process took place from RhB to NiB with the NIR fluorescence emission at 680 nm and a high energy transfer efficiency of 80%. Therefore, the present supramolecular cascade assembly was excited by the two-photon to give NIR fluorescence, which was successfully applied in mitochondria targeted cancer cell labeling.

College of Chemistry, State Key Laboratory of Elemento-Organic Chemistry, Nankai University, Tianjin 300071, P. R. China. E-mail: yuliu@nankai.edu.cn

† Electronic supplementary information (ESI) available: Details of synthetic route, characterization data, and UV-vis absorbance and fluorescence spectra. See DOI: https://doi.org/10.1039/d3cc03487a

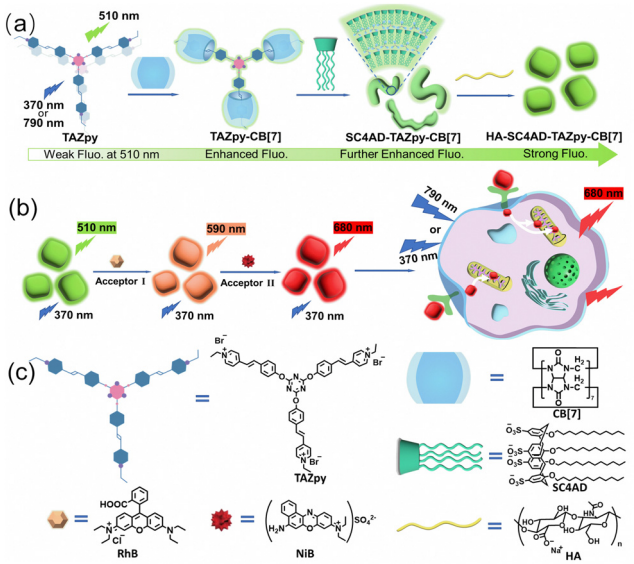

Scheme 1 Schematic illustration of (a) the construction of supramolecular nanoparticles HA-SC4AD-TAZpy-CB[7] in aqueous solution; (b) the formation of a two-step sequential fluorescence harvesting system with NIR emission for two-photon excitation mitochondria targeted imaging of HeLa cells; (c) chemical structures of the compounds.

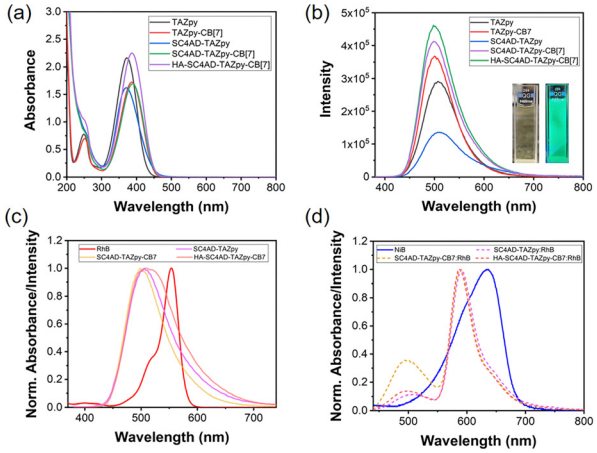

Fig. 1 (a) UV-vis absorbance and (b) fluorescence spectra of TAZpy, TAZpy-CB[7], SC4AD-TAZpy, SC4AD-TAZpy-CB[7] and HA-SC4AD-TAZpy-CB[7]; (c) normalized absorption spectra of RhB and emission spectra of SC4AD-TAZpy, SC4AD-TAZpy-CB[7], and HA-SC4AD-TAZpy-CB[7]; (d) normalized absorption spectra of NiB and emission spectra of SC4AD-TAZpy:RhB, SC4AD-TAZpy-CB[7]:RhB, and HA-SC4AD-TAZpy-CB[7]:RhB.

The triazine derivative with a three-armed pyridinium (TAZpy) was prepared by the reaction of 2,4,6-tris(4-formylphenoxy)-1,3,5-triazine (TAZ) and 1-ethyl-4-methylpyridinium bromide (Scheme S1, ESI†), which was characterized by nuclear magnetic resonance (NMR) and high-resolution mass spectrometry (HR-MS) in Fig. S1–S4 (ESI†). The binding behaviour between TAZpy and CB[7] was investigated by UV-vis spectroscopy (Fig. S5, ESI†). The apparent binding constant (K_{obs}) was determined to be 1.37×10^5 M^{-1} in TAZpy-CB[7] by the nonlinear least-squares fitting method and the stoichiometry of the inclusion complex was measured to be 1 : 3 of TAZpy : CB[7] by the Job's plot, which may be ascribed to the pyridinium units of TAZpy being included by the host CB[7] to form a TAZpy-CB[7] complex (Fig. S6, ESI†). The resultant 1 : 3 binary species TAZpy-CB[7] was evaluated by ^{1}H NMR contrast experiments in D_2O (Fig. S7, ESI†). The chemical shift of pyridinium moved upfield, which supported that the guest TAZpy was encapsulated into the hydrophobic cavity of CB[7]. SC4AD was employed to assemble with TAZpy-CB[7], which formed SC4AD-TAZpy-CB[7] nanofibers to achieve the further enhancement of the fluorescence emission at 510 nm based on the macrocyclic confinement. In the absence of CB[7], the induced aggregation behaviour of amphiphilic SC4AD toward TAZpy was also investigated by optical transmittance (Fig. S8, ESI†).[7] The optical transmittance of the free TAZpy at 600 nm was nearly unchanged with the concentration increasing from 0 to 6×10^{-5} M, which indicated that TAZpy could not self-aggregate in the concentration range. In the presence of SC4AD, the optical transmittance was decreased rapidly with the increase of the TAZpy concentration, and the calculated critical aggregation concentration (CAC) value of TAZpy was 1.78×10^{-5} M, suggesting that SC4AD can effectively induce the aggregation of TAZpy to form supramolecular SC4AD-TAZpy nanoparticles through electrostatic interaction. According to the calculation of CAC, the preferable mixing molar ratio between SC4AD and TAZpy was also evaluated as 1 : 1 (Fig. S9, ESI†). Without the macrocyclic confinement of CB[7], the fluorescence emission of TAZpy was quenched obviously when assembled with SC4AD, which demonstrated that the host CB[7] was essential for improving luminescence performance.

Moreover, SC4AD-TAZpy-CB[7] can also cascade assemble with negative HA to further enhance the fluorescence intensity *via* electrostatic interaction. The fluorescence emission at 510 nm was the highest when the concentration of HA added into SC4AD-TAZpy-CB[7] solution reached 10 μg mL^{-1} (Fig. S10, ESI†). As shown in Fig. 1a and b, the changes of the absorption spectra and fluorescence spectra demonstrated that the three-armed vinyl pyridinium moieties of TAZpy were encapsulated into the cavity of CB[7] to enhance the fluorescence emission based on the macrocycle confinement avoiding the fluorescence quenching, and the formed supramolecular cascade assembly HA-SC4AD-TAZpy-CB[7] showed relatively strong fluorescence emission at 510 nm. Compared with TAZpy and TAZpy-CB[7], the mixture solutions of SC4AD-TAZpy, SC4AD-TAZpy-CB[7] and HA-SC4AD-TAZpy-CB[7] at the optimal assembly ratio displayed a clear Tyndall effect, which proved the formation of abundant and stable supramolecular assemblies (Fig. S11, ESI†). Meanwhile, the time-resolved PL decay curve analysis demonstrated that the fluorescence lifetimes all stayed in the nanosecond level at 510 nm (Fig. S12, ESI†). The fluorescence quantum yields of TAZpy, TAZpy-CB[7], SC4AD-TAZpy, and SC4AD-TAZpy-CB[7] were measured to be 1.26%, 1.32%, 0.66% and 1.44%, respectively. In contrast, the quantum yield of HA-SC4AD-TAZpy-CB[7] displayed an enhancement of 2.00% because of the macrocyclic confinement and cascade assembly (Fig. S13, ESI†). Zeta potential, dynamic light scattering (DLS), transmission electron microscopy (TEM) and

scanning electron microscopy (SEM) experiments have also been performed to confirm the formation of the supramolecular assemblies (Fig. S14–S17, ESI†).

HA-SC4AD-TAZpy-CB[7] possessing an inner hydrophobic layer and excellent optical performance was beneficial to co-assemble with suitable dye molecules to construct an efficient cascade FRET platform to realize NIR luminescence.[8] Rhodamine B (RhB), a kind of fluorescent dye with high fluorescence quantum yield, was selected as the primary acceptor.[9] Not only the absorption band of RhB have an adequate overlap with the emission of HA-SC4AD-TAZpy-CB[7] (Fig. 1c), but also RhB could be easily encapsulated into the internal close-packed structure of HA-SC4AD-TAZpy-CB[7] assembly through the hydrophobic effect satisfying the short distance requirement between the donor and the acceptor. With the continuous addition of RhB (acceptor I) to the HA-SC4AD-TAZpy-CB[7] assembly (donor I), the fluorescence emission at 510 nm quenched gradually while the fluorescence emission of RhB at 590 nm appeared and increased. When the ratio of donor I to acceptor I reached 50 : 1, the fluorescence spectral changes reached an equilibrium state, and Φ_{ET1} was calculated as 48% indicating that there was an effective FRET process taking place from HA-SC4AD-TAZpy-CB[7] to RhB (Fig. 2a and b). Thus, the possibility of the secondary energy transfer of HA-SC4AD-TAZpy-CB[7]:RhB was explored. The HA-SC4AD-TAZpy-CB[7] supramolecular assembly possesses negative zeta potential, which is favourable for loading a NIR emissive organic dye NiB with positive charge *via* electrostatic interaction and hydrophobic effect in aqueous solution.[10] NiB with NIR emission was adopted as the second acceptor to investigate the fluorescence cascade energy transfer process because of the valid spectral overlap between the emission band of HA-SC4AD-TAZpy-CB[7]:RhB and the absorption band of NiB (Fig. 1d). When the NiB (acceptor II) was introduced into the HA-SC4AD-TAZpy-CB[7]:RhB system (donor II), the fluorescence emission of RhB at 590 nm decreased and a new emission peak at 680 nm appeared and enhanced continuously under 370 nm excitation. It is worth noting that the intensity of the HA-SC4AD-TAZpy-CB[7] assembly at 510 nm remains almost constant, indicating that the energy of HA-SC4AD-TAZpy-CB[7] has been greatly quenched in the first-order energy transfer process and the spectral overlap of the original donor and NiB is very small. As shown in Fig. 2c and d, the NIR emission of NiB was readily observed in the presence of a trace amount of NiB and an efficient secondary fluorescence energy transfer process with high efficiency up to 80% (Φ_{ET2}) took place achieving a large Stokes shift (310 nm) when the molar ratio of HA-SC4AD-TAZpy-CB[7] : RhB : NiB reached 3000 : 60 : 15 (Fig. S18, ESI†).

The SC4AD-TAZpy and SC4AD-TAZpy-CB[7] assemblies can also exhibit cascade energy transfer in aqueous solution (Fig. S19, ESI†). When the donors/acceptor I ratios came to 20 : 1 and 40 : 1, the first-order energy transfer process reached equilibrium and the Φ_{ET1} was calculated as 25% (SC4AD-TAZpy:RhB) and 42% (SC4AD-TAZpy-CB[7]:RhB), respectively. With the further addition of acceptor II, the secondary FRET efficiency of the SC4AD-TAZpy : RhB : NiB and SC4AD-TAZpy-CB[7] : RhB : NiB systems were determined correspondingly to be 53% and 70% when the ratios of donor to acceptor were up to 3000 : 150 : 15 and 3000 : 75 : 40, which were both lower than Φ_{ET2} (80%) of the HA-SC4AD-TAZpy-CB[7] : RhB : NiB system (Fig. S20, ESI†). The reason for the lower energy transfer efficiency may be from the less spectral overlap of RhB and the SC4AD-TAZpy and SC4AD-TAZpy-CB[7] assemblies (Fig. 2c) and the lower quantum yield than that of the HA-SC4AD-TAZpy-CB[7] assembly. Given the above results, the HA-SC4AD-TAZpy-CB[7] assembly could act as an ideal donor for establishing a cascade energy capturing scaffold in aqueous solutions.

Given the satisfactory fluorescence performance and the cancer cell targeting, we applied the HA-SC4AD-TAZpy-CB[7] supramolecular cascade assembly in cell-imaging experiments. The cytotoxicity of the system was evaluated toward human cervical carcinoma cells (HeLa cells), human lung adenocarcinoma cells (A549 cells) and normal human embryonic kidney cells (293T cells) *via* a Cell Counting Kit-8 assay (Fig. S21, ESI†). The results demonstrated that the viability of HeLa and A549 cells could still remain above 90% after 24 h of incubation with HA-SC4AD-TAZpy-CB[7] ranging from 0 to 3.5×10^{-5} M, and the 293T cell survival rate remained above 80%, which indicated that the nanoaggregates had low cytotoxicity. Meanwhile, the subcellular localization of the HA-SC4AD-TAZpy-CB[7] supramolecular assembly was probed by employing a commercial mitochondrion marker Mito-Tracker Red utilizing confocal laser scanning microscopy (Fig. S22, ESI†). HeLa and A549 cells both exhibited bright green signals and overlapped well with the red signal of Mito-Tracker Red as shown by the emergence of yellow areas in the merged images, illustrating that such assembly possessed the specific mitochondrion-targeting ability of cancer cells. On the other hand, almost no green emission signal was found in 293T cells, which indicated

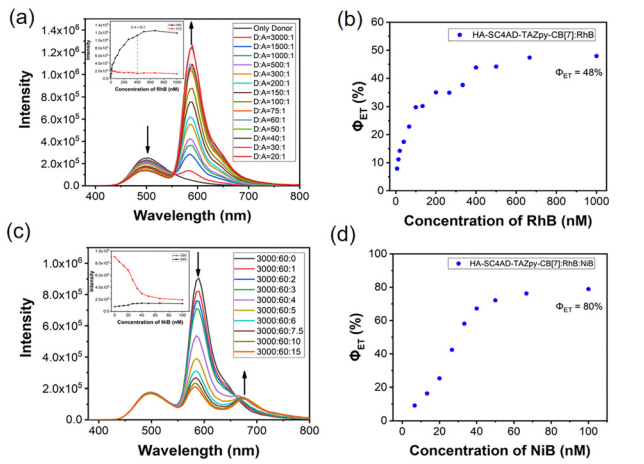

Fig. 2 (a) Fluorescence spectra and (b) Φ_{ET1} of HA-SC4AD-TAZpy-CB[7] : RhB at different donor/acceptor ratios (inset: fluorescence intensity changes at 510 nm and 590 nm); (c) fluorescence spectra and (d) Φ_{ET2} of HA-SC4AD-TAZpy-CB[7] : RhB : NiB at different donor/acceptor ratios (inset: fluorescence intensity changes at 590 nm and 680 nm) ([HA] = 10 μg mL^{-1}, [SC4AD] = [TAZpy] = 2×10^{-5} M, [CB[7]] = 6×10^{-5} M, λ_{ex} = 370 nm).

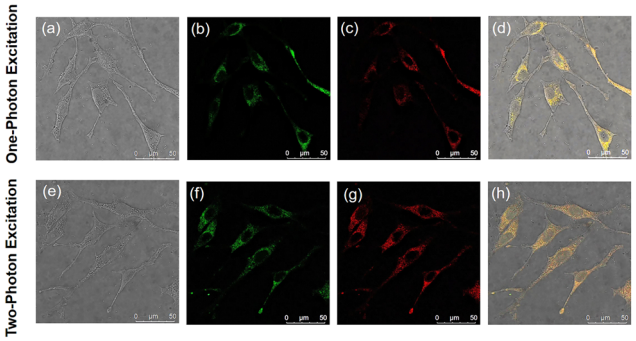

Fig. 3 CLSM images of HeLa cells incubated with HA-SC4AD-TAZpy-CB[7]:RhB:NiB excited at 405 nm: (a) bright field, (b) green channel (480–560 nm), (c) red channel (620–720 nm) and (d) the merged image of (a)–(c); two-photon microscopic images of HeLa cells incubated with HA-SC4AD-TAZpy-CB[7] : RhB : NiB excited at 790 nm: (e) bright field, (f) green channel, (g) red channel and (h) the merged image of (e)–(g).

that HA-SC4AD-TAZpy-CB[7] was preferentially internalized by cancer cells than normal cells due to HA receptor targeting mediated endocytosis.[11]

Interestingly, the supramolecular assembly HA-SC4AD-TAZpy-CB[7] exhibited two-photon excitation property (Fig. S23, ESI†). The excitation wavelength of HA-SC4AD-TAZpy-CB[7] ranged from 745 nm to 950 nm measured by femtosecond laser pulses. The maximum emission peak of the fluorescence spectrum of HA-SC4AD-TAZpy-CB[7] under two-photon excitation at 790 nm is similar to that excited at 370 nm. Benefiting from the capability of two-photo excitation and mitochondria targeted cancer cell imaging, the intracellular distribution of the HA-SC4AD-TAZpy-CB[7]:RhB:NiB light capturing system was investigated by two-photon and confocal laser scanning microscopy (CLSM). Both green and NIR red luminescence was observed in the cytoplasm of HeLa cells under a 405 nm (one-photo excitation) and 790 nm (two-photo excitation) femtosecond pulsed laser, which overlapped well showing the merged yellow dyeing sites (Fig. 3). The above results illustrated that the HA-SC4AD-TAZpy-CB[7]:RhB:NiB supramolecular system possessed NIR emission and low cytotoxicity under the NIR light irradiation in biological targeting imaging research, which could avoid the interference from autofluorescence and background fluorescence compared with the traditional cell dyes.[12]

In summary, we constructed an excellent light capturing supramolecular cascade assembly based on TAZpy, CB[7], SC4AD, HA, RhB and NiB through the host–guest and electrostatic interactions and π–π stacking effect in aqueous solution. CB[7] encapsulated TAZpy to form a 1 : 3 TAZpy-CB[7] complex with an enhancement of fluorescence intensity due to the macrocyclic confinement, and then cascade assembled with SC4AD and HA *via* electrostatic interaction to form nanoparticles achieving fluorescence with further cascade increase. The obtained HA-SC4AD-TAZpy-CB[7] served as an efficient FRET platform to RhB and NiB with a high efficiency of 80%, displaying NIR fluorescence emission at 680 nm. Meanwhile, the HA-SC4AD-TAZpy-CB[7]:RhB:NiB system was successfully applied in two-photon NIR mitochondria targeted cancer cell imaging. This novel supramolecular system exhibits the advantages of NIR emission, low phototoxicity and mitochondrial targeting, and solves the problem of short excitation and emission wavelengths, which provides an efficient method for application in bioimaging.

This work was financially supported by the National Natural Science Foundation of China (grant 22131008).

Conflicts of interest

There are no conflicts to declare.

Notes and references

1 (*a*) Y. Sun, F. Guo, T. Zuo, J. Hua and G. Diao, *Nat. Commun.*, 2016, **7**, 12042; (*b*) Z.-X. Liu and Y. Liu, *Chem. Soc. Rev.*, 2022, **51**, 4786; (*c*) J. Niu, Y.-H. Liu, W.-S. Xu, W.-W. Xu, Y.-H. Song, J. Yu, Y.-M. Zhang and Y. Liu, *Chem. Commun.*, 2023, **59**, 4680; (*d*) X. Zhao, Y. Chen, X.-Y. Dai, W.-L. Zhou, J.-J. Li and Y. Liu, *Adv. Photonics Res.*, 2020, **1**, 2000007.
2 (*a*) H.-G. Nie, Z. Wei, X.-L. Ni and Y. Liu, *Chem. Rev.*, 2022, **122**, 9032; (*b*) G. Wu, Z. Huang and O.-A. Scherman, *Angew. Chem., Int. Ed.*, 2020, **59**, 15963; (*c*) X. Ma and H. Tian, *Acc. Chem. Res.*, 2014, **47**, 1971; (*d*) Q.-M. Lin, L.-Y. Li, M. Tang, S. Uenuma, J. Samanta, S.-D. Li, X.-F. Jiang, L.-Y. Zou, K. Ito and C.-F. Ke, *Chem*, 2021, **7**, 2442; (*e*) H.-T.-T. Zhu, L.-Q. Shangguan, B.-B. Shi, G.-C. Yu and F.-H. Huang, *Mater. Chem. Front.*, 2018, **2**, 2152.
3 (*a*) W.-L. Zhou, X. Zhao, Y. Chen and Y. Liu, *Org. Chem. Front.*, 2019, **6**, 10–14; (*b*) X.-K. Ma and Y. Liu, *Acc. Chem. Res.*, 2021, **54**, 3403; (*c*) H.-Y. Tian, X.-K. Yu, J.-B. Yao., G.-W. Gao, W.-H. Wu and C. Yang, *Chem. Commun.*, 2021, **57**, 1806; (*d*) X.-Y. Lou and Y.-W. Yang, *Adv. Mater.*, 2020, **32**, 2003263.
4 (*a*) T.-X. Xiao, W.-W. Zhong, L. Zhou, L.-X. Xu, X.-Q. Sun, R.-B.-P. Elmes, X.-Y. Hu and L.-Y. Wang, *Chin. Chem. Lett.*, 2019, **30**, 31; (*b*) K.-Y. Wang, K. Velmurugan, B. Li and X.-Y. Hu, *Chem. Commun.*, 2021, **57**, 13641.
5 S. Garain, B.-C. Garain, M. Eswaramoorthy, S.-K. Pati and S.-J. George, *Angew. Chem., Int. Ed.*, 2021, **60**, 19720.
6 M.-D. Tian, Z. Wang, X. Yuan, H. Zhang, Z.-X. Liu and Y. Liu, *Adv. Funct. Mater.*, 2023, **33**, 2300779.
7 (*a*) Y.-X. Wang, Y.-M. Zhang and Y. Liu, *J. Am. Chem. Soc.*, 2015, **137**, 4543; (*b*) J.-J. Li, Y. Chen, J. Yu, N. Cheng and Y. Liu, *Adv. Mater.*, 2017, **29**, 1701905.
8 (*a*) M. Hao, G. Sun, M. Zuo, Z. Xu, Y. Chen, X.-Y. Hu and L. Wang, *Angew. Chem., Int. Ed.*, 2020, **59**, 10095; (*b*) X.-Y. Dai, Y.-Y. Hu, Y. Sun, M. Huo, X. Dong and Y. Liu, *Adv. Sci.*, 2022, **9**, 2200524.
9 (*a*) W.-W. Xing, H.-J. Wang, Z.-X. Liu, Z.-H. Yu, H.-Y. Zhang and Y. Liu, *Adv. Optical Mater.*, 2023, **11**, 2202588; (*b*) F. Jiao, X. Wu, T. Jian, S. Zhang, H. Jin, P. He, C.-L. Chen and J.-J. De Yoreo, *Angew. Chem., Int. Ed.*, 2019, **58**, 12223.
10 X.-M. Chen, Q. Cao, H.-K. Bisoyi, M. Wang, H. Yang and Q. Li, *Angew. Chem., Int. Ed.*, 2020, **59**, 10493.
11 (*a*) X.-Y. Dai, M. Huo, X. Dong, Y.-Y. Hu and Y. Liu, *Adv. Mater.*, 2022, **34**, 2203534; (*b*) Z.-Y. Ma, H.-Y. Han and Y. L. Zhao, *Biomaterials*, 2023, **293**, 121947.
12 (*a*) F.-F. Shen, Y. Chen, X.-F. Xu, H.-J. Yu, H.-R. Wang and Y. Liu, *Small*, 2021, **17**, 2101185; (*b*) Y. Huang, L.-Y. Shen, D.-B. Guo, W. Yasen, Y. Wu, Y. Su, D. Chen, F. Qiu, D.-Y. Yan and X.-Y. Zhu, *Chem. Commun.*, 2019, **55**, 6735; (*c*) M. Pawlicki, H.-A. Collins, R.-G. Denning and H.-L. Anderson, *Angew. Chem. Int. Ed.*, 2009, **48**, 3244.